

## Anti-coking Attributes of Ce-promoted Co-Ni/Al<sub>2</sub>O<sub>3</sub> Catalyst during Propane Dry Reforming

**Faisal M. Althenayan, Adesoji A. Adesina\***

Reactor Engineering & Technology Group, School of Chemical Sciences & Engineering,  
University of New South Wales, Sydney, New South Wales 2052, Australia

\*E-mail: [a.adesina@unsw.edu.au](mailto:a.adesina@unsw.edu.au). Phone: +61-2-9385 5268. Fax: +61-2-9385 5966

### ABSTRACT

Dry reforming of propane has been carried out over alumina-supported 5Co-10Ni catalyst promoted with ceria. Catalysts containing different levels of Ce (0-2.5wt%) were prepared via co-impregnation of the metal nitrates. Catalysts were characterised using XRF, liquid N<sub>2</sub> adsorption, XRD, temperature programmed desorption of NH<sub>3</sub> and CO<sub>2</sub> as well as temperature-programmed reduction with H<sub>2</sub>. While BET area and pore volume appeared unaffected by ceria addition, the ratio of the surface acidic-to-basic site concentration decreased to a minimum before levelling off at about 1.5wt%Ce. Carbon deposition was not noticeable in catalysts containing more than 1.5wt% Ce due to increased basicity. Time-on-stream activity measurements also confirmed that the Ce-doped were also more stable. A simple mechanism describing the carbon resilience ability of the Ce-catalyst was proposed and it adequately explained the behaviour of the product selectivity ratio over both doped and unpromoted Co-Ni catalysts. Moreover, this study employed a method originally proposed by Levenspiel (1999) to determine the intrinsic reaction rate simultaneously with the carbon-induced deactivation coefficient from transient rate data over an extended period of time (up to 10 hours) for propane dry reforming over the promoted catalyst carried at feed ratio of CO<sub>2</sub>:C<sub>3</sub>H<sub>8</sub>, 0.75 and 1.5. The rate constant  $k'$  and deactivation coefficient,  $k_d$  were determined from a fit of the concentration history data to the hyperbolic reaction-deactivation model for 1<sup>st</sup> order kinetics in a plug flow reactor. Arrhenius treatment of  $k_d$  shows that the activation energy estimates for the deactivation process,  $E_d$  varied with feed ratio 0.75 (83.5-133.5 kJ mol<sup>-1</sup>) and 1.5 (33.6-45.7 kJ mol<sup>-1</sup>) respectively over the range of Ce loading employed. While the activation energy for reforming reaction,  $E_{rxn}$ , is essentially unchanged with Ce loading at 25 and 48 kJ mol<sup>-1</sup> for feed ratios of 0.75 and 1.5 accordingly.

### INTRODUCTION

Ni-supported catalysts are most commonly used for hydrocarbon reforming (dry or steam) reactions to produce synthesis gas (Zhang and Verykios 1994). Dry reforming utilises CO<sub>2</sub>, a greenhouse gas, as the co-reactant to the hydrocarbon and as a result, the associated reduction in overall plant GHG emission is an incentive for employing this route in syngas production. In particular, it yields relatively low H<sub>2</sub>:CO ratio (<3) which can be directly supplied to a GTL fuels production facility. The reaction is, however, accompanied by significant carbon deposition with potential challenges for on-line catalyst deactivation and pathological reformer operation (such as bed clogging and defluidisation). Bimetallic catalysts generally show better activity, selectivity, and deactivation resistance compared to monometallic catalysts in many hydrocarbon-mediated reactions (Wang et al. 2005; Dias and Assaf 2008).

Moreover, it has been reported catalyst promoted with cerium showed excellent anti-coking attributes and stability (Ma et al. 1996; Trovarelli et al. 2001; Asami et al. 2003). The main aim of this study was to investigate the influence cerium addition to the activity of 5Co:10Ni/85 $\gamma$ -Al<sub>2</sub>O<sub>3</sub> catalyst during CO<sub>2</sub> reforming of propane.

Since the reaction is conventionally carried out over a promoted Co-Ni catalyst at temperature above 773 K. The accompanying carbon deposition often leads to catalyst deactivation and pathological reactor operation. Since both dry reforming and carbon deposition take place concurrently the true reforming reaction rate is continuously masked by on-line catalyst activity decay which is non-separable from the intrinsic kinetics. (Levenspiel 1999) proposed a reaction deactivation coupled rate analysis which permits extraction of the intrinsic rate constant as well as the deactivation coefficient from transient concentration profile of the reactant(s) for 1<sup>st</sup> order reaction kinetics taking place in a plug flow or stirred tanks reactor for different activity decay laws. This analysis was subsequently generalized and extended to other schemes by (Hardiman et al. 2005). In what follows, this method is used to analyse the CO<sub>2</sub> reforming of propane which satisfies the basic features present in coke-induced deactivation of hydrocarbon-mediated reaction.

## EXPERIMENTAL DETAILS

Catalyst activity and kinetic studies were conducted in a 15 mm ID (length = 300 mm) quartz fixed-bed reactor at atmospheric pressure and temperature of 798-973 K. Feed containing CO<sub>2</sub>, C<sub>3</sub>H<sub>8</sub> and Ar at the desired ratio was supplied at 100 ml min<sup>-1</sup> to the reactor loaded with 0.5 g of the catalyst. Catalysts with different cerium content (0-2.5 wt%) in the Co-Ni/Al<sub>2</sub>O<sub>3</sub> were prepared by the co-impregnation method in which the  $\gamma$ -alumina was initially heated at 1073 K for 6 h and then impregnated with aqueous solutions containing quantitative amounts of Co(NO<sub>3</sub>)<sub>2</sub>, Ni(NO<sub>3</sub>)<sub>2</sub>, and Ce(NO<sub>3</sub>)<sub>2</sub> at the desired loading. The addition of each nitrate solution was followed by 3 h of stirring at 303 K and subsequent 8-hour drying of the slurry in an oven at 403 K. The resulting product was calcined at 1073 K for 5 h at a heating rate of 5 K min<sup>-1</sup>. The calcined solid was then crushed and sieved to 180–250  $\mu$ m for reactor studies.

Multipoint BET surface area and pore volume data for all catalysts were obtained by liquid N<sub>2</sub> adsorption at 77 K on Quantachrome Autosorb-1 unit. Spent carbon-containing catalysts were examined using Shimadzu Total Organic Carbon (TOC) Analyzer SM-5000A to determine the total carbon content. Temperature-programmed reduction (TPR) experiments were performed in a ThermoCahn TG-2121 TGA unit. TPR runs were carried out at 973 K with 50% H<sub>2</sub>/Ar mixture using a total gas flow of 55 ml min<sup>-1</sup> with temperature ramping at 10 K min<sup>-1</sup>. NH<sub>3</sub> and CO<sub>2</sub> temperature-programmed desorption (TPD) were done on a Micromeritics AutoChem 2910 at 973 K with 4 heating rates (15, 20, 25, 30 K min<sup>-1</sup>) while H<sub>2</sub> chemisorption was conducted in the same apparatus at 383 K. Catalyst morphology and composition were also determined from X-ray diffraction (XRD) and X-ray fluorescence (XRF) analyses respectively.

## RESULTS AND DISCUSSION

### Catalyst characterization

As may be seen from Table 1, XRF analysis showed that the Co-Ni catalyst contained 4.42wt% Co and 10.82wt% Ni in good agreement with the intended recipe (5wt% Co and 10wt%Ni). The presence of trace quantities of Yb, Gd, Si, Sc and Ca may be due to the original impurities in the AR grade chemicals from Sigma-Aldrich. BET and pore volume

data displayed in Table 2 suggest that the addition of ceria to the Co-Ni /Al<sub>2</sub>O<sub>3</sub> catalyst did not have any marked effect on its porosity or surface area - an indication of negligible increase in crystallite size. In fact, X-ray diffraction patterns (cf. Fig. 1) showed that both ceria-promoted and undoped Co-Ni catalysts contained similar cobalt and nickel oxides, with NiCo<sub>2</sub>O<sub>4</sub> ( $2\theta = 31^\circ$  and  $36.6^\circ$ ) and Co<sub>3</sub>O<sub>4</sub> at  $2\theta = 31.2^\circ$  and  $36.7^\circ$  while NiO is located at  $2\theta = 43.2^\circ$ . The metal aluminates, CoAl<sub>2</sub>O<sub>4</sub> ( $2\theta = 36.7^\circ$ ) as well as NiAl<sub>2</sub>O<sub>4</sub> ( $2\theta = 37^\circ$ ;  $44.8^\circ$ ) exhibited strong intensities but the CeO<sub>2</sub> was identified as a separate oxide phase on the ceria-containing catalyst at  $2\theta = 28.6^\circ$ . H<sub>2</sub> chemisorption data collected at 383 K and detailed in Table 2 revealed that the percentage metal dispersion (0.741-1.10) was not affected by the addition of ceria. Indeed, the crystallite size varied between 93-146 nm and consistent with XRD measurements.

Tab.1: XRF analysis results for 5Co-10Ni/Al<sub>2</sub>O<sub>3</sub>

Metal	Al	Ni	Co	Yb	Gd	Si	Sc	Ca	O <sub>2</sub> (balance)
Content (wt %)	42.44	10.82	4.42	0.521	0.191	0.0566	0.0243	0.0212	41.51

Tab.2: Liquid N<sub>2</sub> physisorption (77 K) and H<sub>2</sub> chemisorption (383 K) results

Ce loading (wt%)	BET Area, S <sub>T</sub> (m <sup>2</sup> g <sup>-1</sup> )	Pore volume, PV (ml g <sup>-1</sup> )	Metal dispersion D (%)	Metal area, S <sub>m</sub> (m <sup>2</sup> g <sup>-1</sup> )	Crystallite size d (nm)
0	121.6	0.526	0.741	0.744	135.84
0.5	117.7	0.5021	0.695	0.718	146.08
1	120.3	0.524	1.100	1.167	93.04
1.5	116.6	0.5225	0.813	0.886	126.74
2	119.7	0.5154	0.801	0.896	129.55
2.5	120.7	0.5449	0.737	0.845	141.86

The profile of the temperature-programmed reduction with H<sub>2</sub> shown in Fig. 2 suggests the presence of nearly identical metal phases in both types of catalyst. The peak at 401 K may be attributed to the removal of interstitial water. The principal broad peak at about 725 K is due to the reduction of a key metal oxide phase containing Co<sub>3</sub>O<sub>4</sub>, NiCo<sub>2</sub>O<sub>4</sub> and NiO. However, the low temperature shoulder peaks (473 to 513 K) are ascribed to the presence of XRD-amorphous Ni<sub>2</sub>O<sub>3</sub> and Co<sub>2</sub>O<sub>3</sub> while the higher temperature peaks suggest the reduction of the metal aluminates (at 973 K). CeO<sub>2</sub> is essentially unreduced below 1000 K.

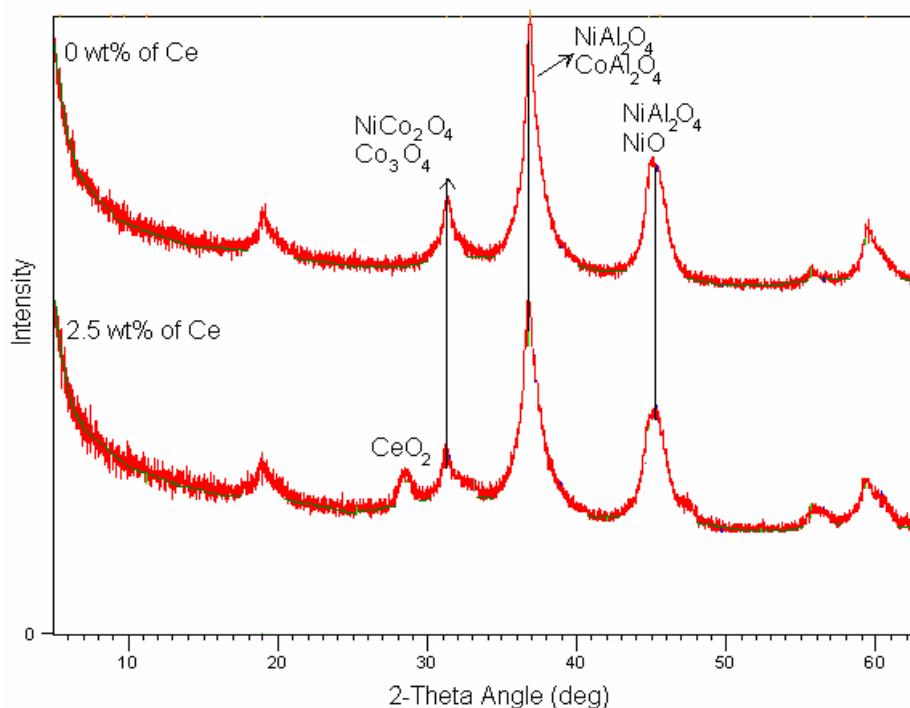


Fig. 1: X-ray patterns for the Co-Ni catalyst and the Ce-promoted counterpart.

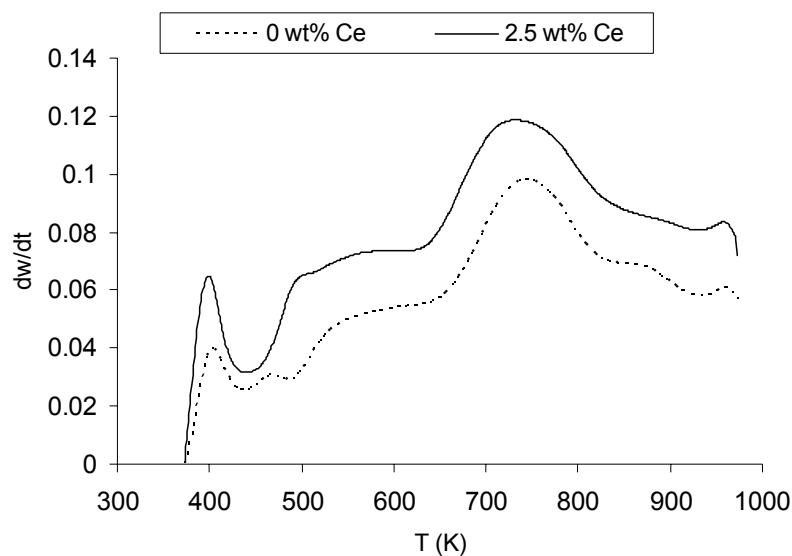


Fig. 2: Thermal spectra for 0 and 2.5wt % Ce-5Co:10Ni catalyst samples at 973K

The results of  $\text{NH}_3$ -TPD summarised in Table 3 indicate that both catalysts have relatively weak acid sites ( $724\text{--}822 \mu\text{mol g}^{-1}$ ) with an  $\text{NH}_3$  heat of desorption,  $E_d$ , of about  $90 \text{ kJ mol}^{-1}$  typical of Lewis acid sites since Bronsted acid sites are generally characterised by  $E_d$  values of  $125\text{--}145 \text{ kJ mol}^{-1}$  (Yaluris et al. 1996). However, the  $\text{CO}_2$ -TPD data portrayed in Table 3 implicate the stronger basic character of the ceria-containing catalyst with heat of  $\text{CO}_2$  desorption,  $E_d$ , values ( $195\text{--}412 \text{ kJ mol}^{-1}$ ) greater than that for the unpromoted Co-Ni catalyst ( $141 \text{ kJ mol}^{-1}$ ). Interestingly, the surface density of these basic sites was also higher in the promoted catalysts and seemed to increase with Ce content.

Tab.3: Summary analysis for NH<sub>3</sub> and CO<sub>2</sub> TPD runs carried out at 973 K and various heating rates (15-30 K min<sup>-1</sup>)

Ce loading wt%	Acidic Site Concentration (mol g <sup>-1</sup> ) x10 <sup>4</sup>	Basic Site Concentration (mol g <sup>-1</sup> ) x10 <sup>5</sup>	Acidic:Basic Site Ratio	Heat of desorption for NH <sub>3</sub> , E <sub>a</sub> , (kJ mol <sup>-1</sup> )	Heat of desorption for CO <sub>2</sub> , E <sub>a</sub> , (kJ mol <sup>-1</sup> )
0	8.209	2.307	35.582	90.71	141.26
0.5	7.724	3.715	20.788	90.44	411.79
1	7.465	3.542	21.074	101.86	201.96
1.5	7.245	3.702	19.571	97.35	196.13
2	8.223	4.072	20.193	89.74	195.13
2.5	7.342	4.268	17.203	87.90	209.93

### Catalyst Activity and Kinetic Analysis

Figs. 3 (a-b) plot the reaction rate as a function of the Ce content in the catalyst. Both H<sub>2</sub> and CO production rate increased with Ce addition attaining a plateau at 1.5 wt% Ce. It is also evident from these data that the addition of ceria promotes CO<sub>2</sub> consumption rate but levelled off at the same Ce loading. Conversely, the CH<sub>4</sub> production rate decreased almost linearly with Ce loading and flattened out beyond critical value of 1.5 wt% Ce. The promotional effect of ceria in steam reforming catalysts has been attributed to its oxygen storage capacity due to the stability and flexibility in the +3 and +4 oxidation states for Ce (Asami et al. 2003). There has, however, been no attempt (Ma et al. 1996; Kugai et al. 2006) to systematically evaluate the behaviour with ceria loading to obtain quantitative insights. In particular, many of these studies have only dealt with steam reforming and very little has been reported in the open literature with respect to ceria effect during dry reforming operation.

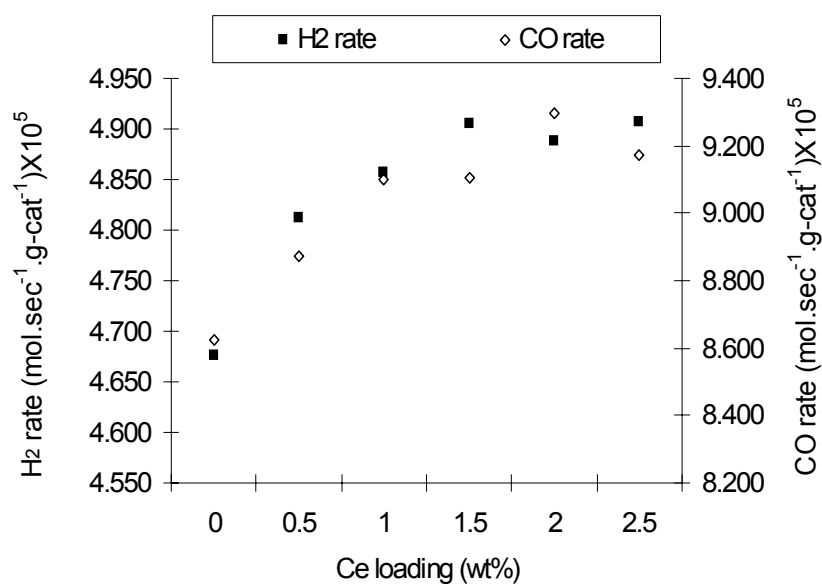


Fig. 3a: H<sub>2</sub> and CO production rates vs Ce loading for at 923 K and CO<sub>2</sub>:C<sub>3</sub>H<sub>8</sub> = 5.0

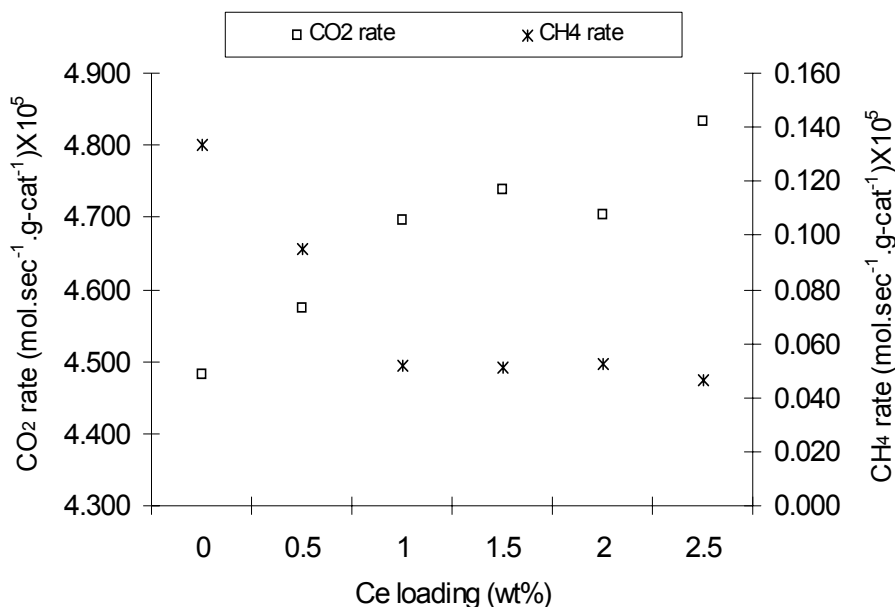


Fig. 3b: CH<sub>4</sub> production and CO<sub>2</sub> consumption rates vs Ce loading at 923 K and CO<sub>2</sub>:C<sub>3</sub>H<sub>8</sub> = 5.0

Fig. 4 represents the TOC concentration for the spent catalysts from reaction under a CO<sub>2</sub>:C<sub>3</sub>H<sub>8</sub> ratio = 5 at 923 K. The data revealed the beneficial effect of ceria addition to the bimetallic catalyst especially when the Ce content is higher than 1.5 wt%.

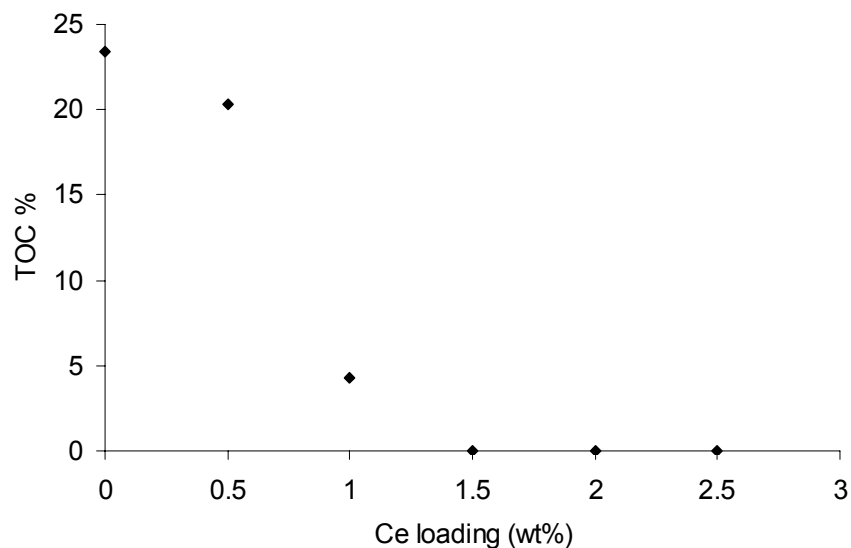


Fig. 4: TOC results for used ceria-promoted catalysts.

This behaviour may be adequately described by the sigmoid function:

$$TOC (\%) = \frac{a}{1 + e^{-\left(\frac{y_{Ce} - c}{b}\right)}} \quad (1)$$

where  $y_{Ce}$  is the Ce loading (%), 'a' is the carbon deposition capacitance of the unpromoted Co-Ni catalysts, 'b' is the anti-coking factor Ce and 'c' is the critical Ce loading for which the carbon capacitance of the unpromoted catalyst is halved. Nonlinear regression of the data (using POLYMATH 5.2) gave parameter estimates for  $a$ ,  $b$  and  $c$  as: 23.55 %, -0.1501, and 0.7754 wt% Ce, respectively.

The resistance to carbon deposition beyond Ce loading of 1.5 wt % is consistent with the "plateau" seen in the H<sub>2</sub>, CO and CO<sub>2</sub> rates in Figs. 3. Incidentally, CH<sub>4</sub> rate also dropped with increased Ce content remaining practically invariant beyond this crucial point (cf. Fig. 3b). Since CH<sub>4</sub> and carbonaceous deposit are normally co-products of the hydrocarbon dehydrogenation during reforming, the initial decrease in CH<sub>4</sub> formation rate suggests that it was consumed via another pathway (or site) on the ceria-promoted catalyst which was not available on the un-doped Co-Ni catalyst. Indeed, the variation in the acidic:basic site concentration ratio with Ce content (shown in Table 3) is parallel to the trend observed for the CH<sub>4</sub> production rate. In fact, transient reaction data show that the Ce-doped catalysts were stable after the first 1 hour on-stream while CH<sub>4</sub> production (indication of carbon laydown) from the un-promoted Co-Ni catalyst continued to increase even after 5 hours of operation. The most stable catalyst was the 2.5wt% Ce catalyst as seen in Fig. 5.

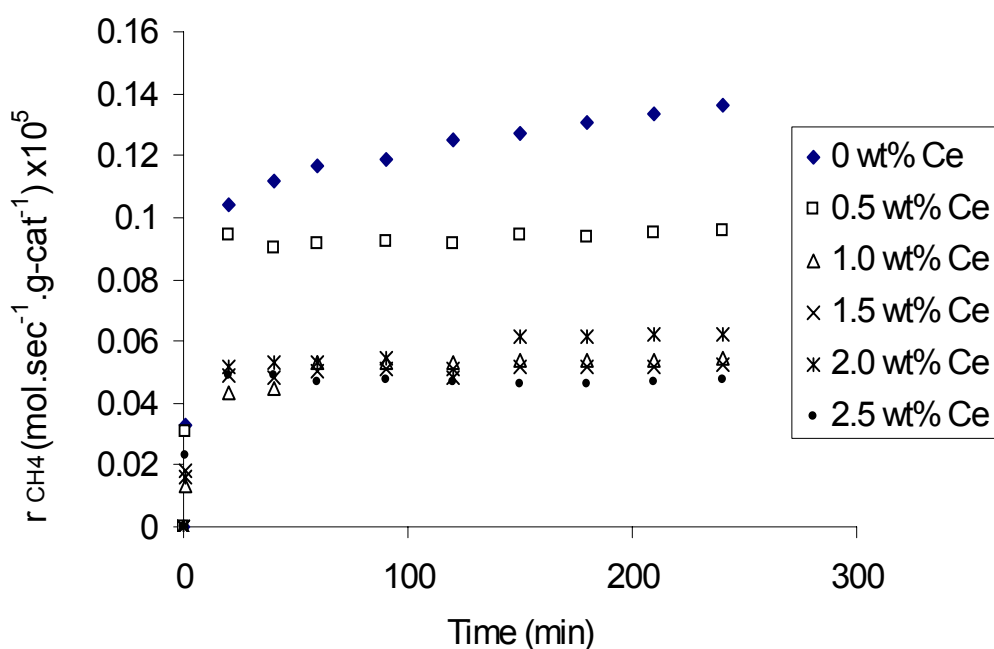
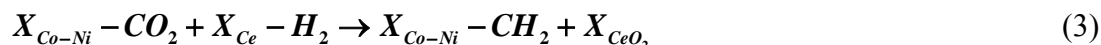


Fig. 5: Transient CH<sub>4</sub> production rate results for runs carried out at 923 K and CO<sub>2</sub>:C<sub>3</sub>H<sub>8</sub> = 5.0

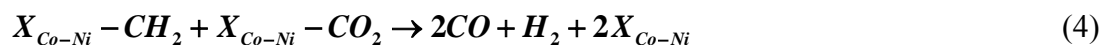
This confirms that the improvement in carbon resilience was due to the increase in surface basic site concentration in the promoted catalyst. It may therefore be proposed that on the ceria catalyst, a secondary route for methane depletion is provided via:



where  $X_{CeO_2}$  is an oxygen-containing surface ceria site and  $X_{Ce-H_2}$  is a lower oxidation state Ce site containing adsorbed hydrogen the while accompanying increase in  $CO_2$  consumption rate (cf. Fig. 3b) may be attributed to the re-oxidation of the Ce-site through



and



where  $X_{Co-Ni}-CO_2$  is the surface adsorbed  $CO_2$  on a Co-Ni catalyst site,  $X_{Co-Ni}$ , and  $X_{CeO_2}$  is the regenerated ceria site. The increase in both  $H_2$  and CO production rates seen in Fig. 3a is consistent with the sequence of steps in Eqs. (1) to (3) and the attainment of a plateau in rate may be due to limitation in surface  $CeO_2$  site concentration and hence,  $CH_4$  adsorption on the ceria catalyst. The reaction rate versus Ce content ( $\theta$ ) behaviour for  $H_2$ , CO and  $CO_2$  may be represented by a Langmuir-type model for a surface adsorption-reaction as:

$$r_i - r_i^o = \frac{a\theta}{1+b\theta} \quad (5)$$

where  $r_i = H_2$  or CO production rate or ( $-r_i$ ) for  $CO_2$  consumption rate and the superscript 'o' indicates rate value in the Ce-free catalyst. Linear regression of the rate data to Eqn (5) yields the Ce-enhancement coefficient,  $a$  and the Ce-surface capacitance,  $b$ , for each species. The data in all cases showed good fit to Eqn (5) with correlation coefficients between 0.966 to 0.981. Table 4 contains the estimates of  $a$  and  $b$ . Based on these findings, subsequent kinetic experiments were conducted on a catalyst containing 2.5wt% Ce to ensure that the benefits of the carbon resilience characteristics of the catalyst were harnessed since  $CO_2:C_3H_8$  ratio values below and above the stoichiometric requirement will be examined for kinetic studies.

Tab.4: Estimates of  $a$  and  $b$  parameters in Eqn. (5)

Species	$a \times 10^3$ (mol g <sup>-1</sup> s <sup>-1</sup> )	$b \times 10^3$
CO <sub>2</sub>	0.214	0.231
CO	0.661	0.617
H <sub>2</sub>	0.529	1.861

The effect of  $CO_2:C_3H_8$  ratio (5 below and 7 above the stoichiometric value of 3) was investigated at 923 K. In general, product distribution was a function of the feed composition. While  $H_2$  and CO were produced for all feed compositions employed,  $CH_4$ ,  $C_2H_4$ ,  $C_2H_6$  and  $C_3H_6$  were observed only at sub-stoichiometric  $CO_2:C_3H_8$  ratios. These hydrocarbons appeared to be the products of propane dehydrogenation and thus, decreased exponentially with increased  $CO_2:C_3H_8$  ratio as seen in Fig. 6a reflecting their reactivity with adsorbed  $CO_2$ .

However,  $H_2$  and CO rate profiles shown in Fig. 6b, initially increased with  $CO_2:C_3H_8$  ratio and exhibited a maximum at value of 3 before a rather gentle decrease at higher values.  $CO_2$  consumption rate profile also followed this trend suggesting that chemisorbed  $CO_2$  was probably used to re-oxidise the reduced site following CO formation and desorption.

The rate behaviour for hydrocarbon production was fitted to the exponential decay law:

$$r_{HC_i} = r_{HC_i}^0 e^{-b_i \alpha} \quad (7)$$

where  $\alpha$  is the  $CO_2:C_3H_8$  ratio and the pre-exponential coefficient,  $r_{HC_i}^0$  corresponds to the formation rate of hydrocarbon species,  $i$ , from direct propane dehydrogenation. A fit of the data to Eqn (7) yielded the parameters in Table 5.

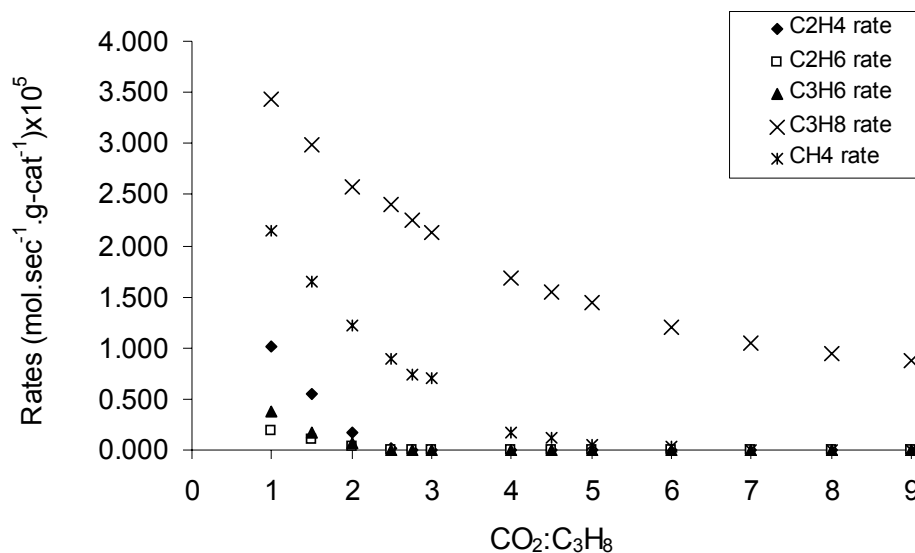


Fig. 6a: Hydrocarbon production rates and C<sub>3</sub>H<sub>8</sub> consumption rate for dry reforming runs on 2.5 wt%Ce-promoted Co-Ni/alumina catalyst at 923K

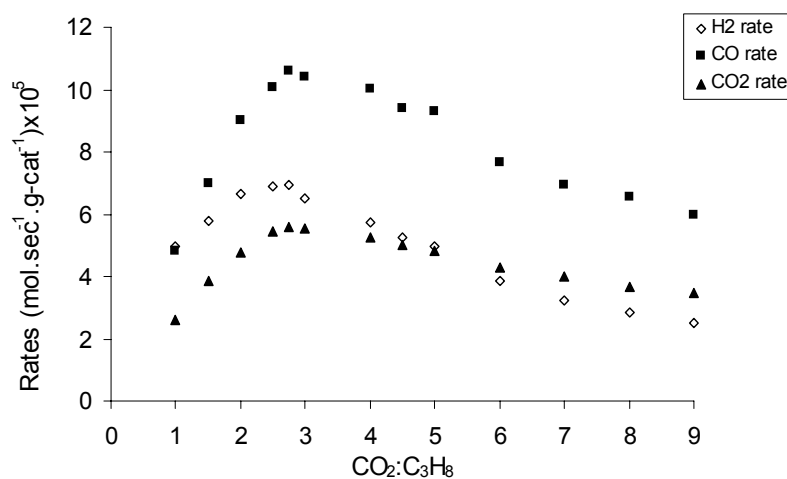


Fig. 6b: H<sub>2</sub> and CO production rates and CO<sub>2</sub> consumption rate during propane dry reforming runs on 2.5 wt%Ce-promoted Co-Ni/alumina catalyst at 923K

Tab.5: Estimates of  $r_{HC_i}^0$  and  $b$  parameters for Eqn. (7)

Species	$r_{HC_i}^0 \times 10^5$ (mol g <sup>-1</sup> s <sup>-1</sup> )	$b$
<b>CH<sub>4</sub></b>	9.650	1.021
<b>C<sub>2</sub>H<sub>4</sub></b>	20.300	2.613
<b>C<sub>2</sub>H<sub>6</sub></b>	0.872	1.519
<b>C<sub>3</sub>H<sub>6</sub></b>	2.347	1.809
<b>C<sub>3</sub>H<sub>8</sub></b>	3.654	0.174

C<sub>2</sub>H<sub>4</sub> and CH<sub>4</sub> have the highest pre-exponential coefficient suggesting that the preferred route for propane dehydrogenation over the catalyst was C<sub>3</sub>H<sub>8</sub> → C<sub>2</sub>H<sub>4</sub> + CH<sub>4</sub>. However, these two products also have the highest and lowest intrinsic reactivity constant,  $b_i$ , (2.61 and 1.02) respectively indicating their roles as the most reactive and most stable hydrocarbons. By same token, the individual rate,  $r_j$ , for H<sub>2</sub>, CO and CO<sub>2</sub> may be described by a Langmuir-Hinshelwood bimolecular surface rate-determining step model;

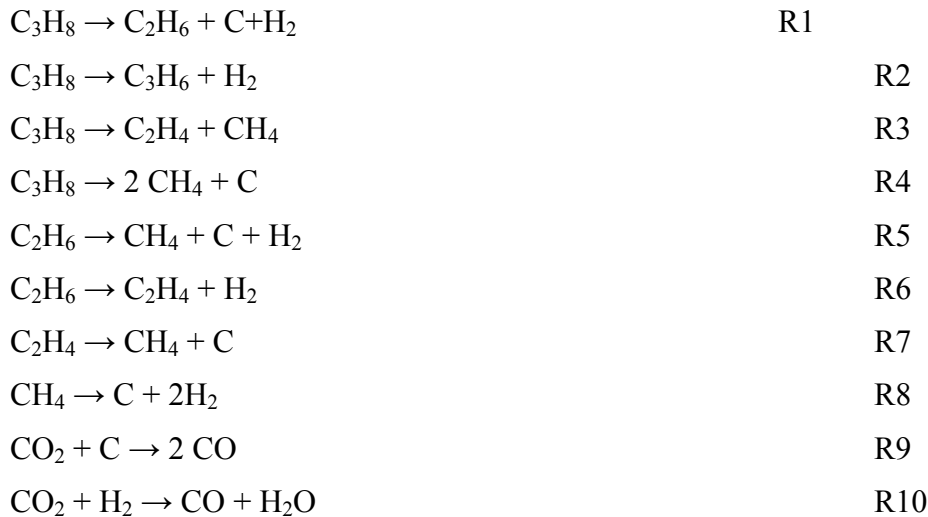
$$r_j = \frac{k_1 \alpha}{(1 + K_2 \alpha)^2} \quad (8)$$

where  $k_1$  and  $K_2$  are kinetic rate and equilibrium adsorption constants respectively. Estimates of the model parameters in Eqn (8) are provided in Table 6 along with the relevant R-squared values confirming the goodness of fit to the data.

Tab.6: Estimates of  $k_1$  and  $K_2$  parameters for Eqn. (8)

Species	$k_1 \times 10^6$ (mol g <sup>-1</sup> s <sup>-1</sup> )	$K_2$	R-squared value
<b>H<sub>2</sub></b>	40.10	1.17	0.984
<b>CO</b>	14.40	0.39	0.976
<b>CO<sub>2</sub></b>	6.99	0.35	0.983

On the strength of these observations, the dry reforming of propane appears to be a complex labyrinth of individual reactions, namely;



However, based on the rank of the matrix of stoichiometric coefficients, only 7 reactions are linearly independent. Since carbon deposition rate,  $r_C$ , and water formation rate,  $r_W$ , were not directly measured via on-line GC analysis, they were determined from a consideration of only the components measured ( $C_3H_8$ ,  $C_3H_6$ ,  $C_2H_6$ ,  $C_2H_4$ ,  $CH_4$ ,  $CO_2$  and  $CO$ ) and  $H_2$  production rate,  $r_{H_2}$ , was used to confirm the validity of the calculations. Thus, the carbon deposition rate,  $r_C$  and water production rate,  $r_W$ , were obtained as:

$$r_C = 3r_{C_3H_8} - 3r_{C_3H_6} - 2r_{C_2H_6} - 2r_{C_2H_4} - r_{CH_4} - r_{CO} + (-r_{CO_2}) \quad (9)$$

$$r_W = 2(-r_{CO_2}) - r_{CO} \quad (10)$$

Table 7 shows that carbon deposition rate decreased with increased  $CO_2$  partial pressure with the negative values simply indicating negligible carbon deposition. Nevertheless, there is no discernible trend in the relationship between water formation rate and  $CO_2:C_3H_8$  ratio probably because water may be involved in other reactions not accounted for in R1 to R10. Product selectivity ratio,  $SR_i$ , (w.r.t. CO) decreased with increased  $CO_2$  in the feed gas as shown in Table 7. Interestingly, the measured  $H_2:CO$  ratio of 0.63 is very close to the theoretical value of 0.67 at the feed composition  $CO_2:C_3H_8$  ratio =3 and further lends credence to confidence in the present analysis.

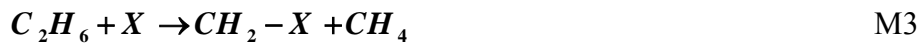
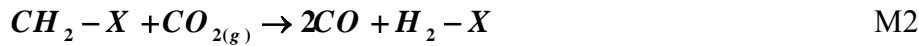
The transient data were fitted to each of the 18 models mentioned in (Hardiman et al. 2005). Discrimination based on the magnitude of the R-squared values ( $R^2 \geq 0.9$ ) revealed that the hyperbolic reaction-deactivation model with  $n=1$  in a plug flow reactor could adequately describe the data at all temperatures and feed compositions used. Transport resistance were negligible with the particle size flow rate reactor diameter used based criteria summarised in (Fogler 1999). Thus, the reaction rate constant,  $k'$  and deactivation coefficient,  $k_d$ , discussed hereafter were estimated from

$$\frac{1}{\ln\left(\frac{C_{A_0}}{C_A}\right)} = \frac{1}{k' \tau'} + \left(\frac{k_d}{k' \tau'}\right) t \quad (11)$$

where  $\tau'$  is space time (g cat. s  $L^{-1}$ ) and defined as  $\tau' = \frac{C_{A_0} W}{F_{A_0}}$ . For experiments carried out

up to 10 hours over the promoted catalyst at feed ratio of  $CO_2:C_3H_8$ , 0.75 and 1.5, the deactivation coefficient,  $k_d$  and the rate constant,  $k'$  were found almost to be fixed with the change in Ce loading. However, Arrhenius treatment of  $E_d$  shows that the activation energy estimates for the true deactivation process,  $E_d$  varied between 83.5-133.5 and 33.6-45.7  $kJ mol^{-1}$ , for feed ratio 0.75 and 1.5 respectively. By same token, the true reforming reaction activity,  $E_{rxn}$ , estimated and found to exhibit insignificant changes for values between 25-48  $kJ mol^{-1}$  for both of the feed ratios of 0.75 and 1.5. Fig. 7 shows one of the results to estimate the  $E_d$  and  $E_{rxn}$  for the run carried out over 0.5 wt% Ce containing catalyst at a feed ratio of 1.5.

These findings suggest at low  $CO_2:C_3H_8$  ratio the catalyst surface will be mostly populated by unsaturated hydrocarbon species with negligible  $CO_2$  coverage and consequently, propane dehydrogenation will be the dominant reaction with relatively low CO production arising from an Eley-Rideal type mechanism. Thus,



Tab. 7: Selectivity ratio estimates, carbon deposition,  $r_C$ , and water formation,  $r_W$ , rate predicted from the proposed reaction network (R1 to R10) for propane dry reforming

CO <sub>2</sub> :C <sub>3</sub> H <sub>8</sub>	SR <sub>H<sub>2</sub></sub>	SR <sub>CH<sub>4</sub></sub>	SR <sub>C<sub>2</sub>H<sub>4</sub></sub>	SR <sub>C<sub>2</sub>H<sub>6</sub></sub>	SR <sub>C<sub>3</sub>H<sub>6</sub></sub>	$r_C \times 10^5$	$r_W \times 10^5$
1	1.038	0.448	0.213	0.038	0.078	2.445	0.433
1.5	0.826	0.235	0.079	0.014	0.024	2.407	0.738
2	0.740	0.135	0.020	0.004	0.007	1.718	0.593
2.5	0.685	0.089	0.002	0.000	0.000	1.638	0.841
2.75	0.654	0.070	0.000	0.005	0.000	0.892	0.608
3	<b>0.628</b>	0.068	0.000	0.011	0.000	0.597	0.694
4	0.574	0.017	0.000	0.016	0.000	-0.247	0.447
4.5	0.559	0.013	0.000	0.063	0.000	-1.062	0.611
5	0.535	0.005	0.000	0.030	0.000	-0.769	0.363
6	0.501	0.004	0.000	0.022	0.000	-0.145	0.918
7	0.462	0.001	0.000	0.014	0.000	-0.024	1.019
8	0.436	0.000	0.000	0.013	0.000	-0.218	0.744
9	0.416	0.000	0.000	0.011	0.000	-0.032	0.950

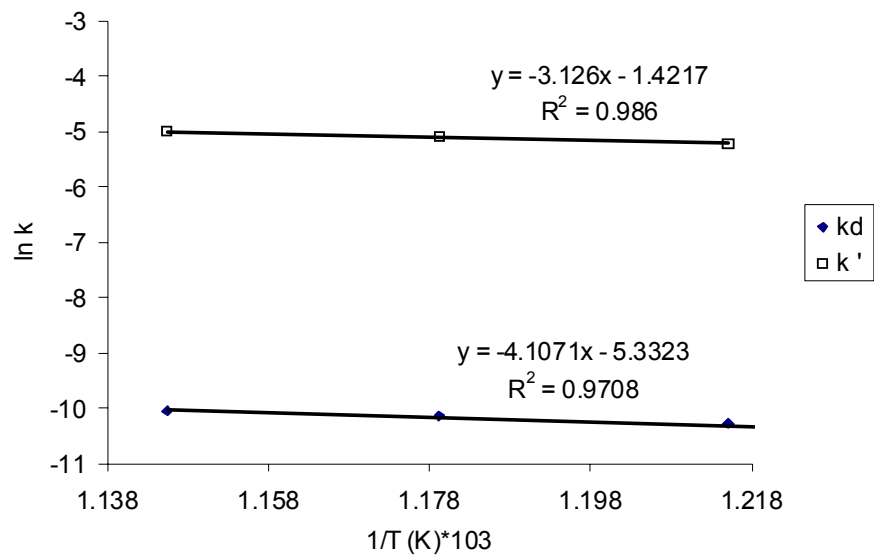


Fig. 7: Arrhenius treatment of  $k_d$  and  $k'$  to estimate the  $E_d$  and  $E_{rxn}$  values. Runs were carried out over 0.5 wt% Ce loading at feed ratio of 1.5

## CONCLUSIONS

This investigation has shown that ceria addition to alumina-supported 5Co-10Ni catalyst helped in mitigating carbon deposition during dry reforming of propane. In particular, the promotional effect appeared to level off at 1.5wt% Ce content. Based on NH<sub>3</sub>- and CO<sub>2</sub>-TPD measurements, the improvement in carbon resilience seems to be due to the increased basicity of Ce-containing catalyst although there was minimal structural difference between the latter and the un-promoted catalyst. A quantitative model describing the effect of Ce promotion for H<sub>2</sub>, CO as well as CH<sub>4</sub> production was obtained. Reaction network analysis using data from the 2.5Ce:5Co:10Ni/alumina catalyst also confirmed that both H<sub>2</sub>:CO ratio and carbon deposition rate decreased with increased CO<sub>2</sub>:C<sub>3</sub>H<sub>8</sub> ratio. Transient analysis shows the catalyst was stable for over 5 days of continuous use with a feed containing CO<sub>2</sub>:C<sub>3</sub>H<sub>8</sub> = 5. Steady-state kinetic modelling revealed that dry reforming has an optimum CO<sub>2</sub> consumption rate as well as H<sub>2</sub> and CO formation rates at about the stoichiometric reactant ratio of CO<sub>2</sub>:C<sub>3</sub>H<sub>8</sub> ratio = 3. C<sub>3</sub>H<sub>8</sub> appeared to be more strongly adsorbed than CO<sub>2</sub> on the catalyst. Arrhenius treatment of  $k_d$  shows that the activation energy estimates for the deactivation process,  $E_d$  varied with feed ratio 0.75 (83.5-133.5 kJ mol<sup>-1</sup>) and 1.5 (33.6-45.7 kJ mol<sup>-1</sup>) respectively over the range of Ce loading employed. While the activation energy for reforming reaction,  $E_{rxn}$ , is essentially unchanged with Ce loading at 25 and 48 kJ mol<sup>-1</sup> for feed ratios of 0.75 and 1.5 accordingly.

## ACKNOWLEDGEMENTS

Financial support of the Australian Research Council is gratefully acknowledged. FMA also appreciates scholarship and study leave from the Saudi Aramco Company.

## REFERENCES

- Asami, K., K. F. X.L., Y. Koyama, A. Sakurama, N. Kometani and Y. Yonezawa (2003). "CO<sub>2</sub> reforming of CH<sub>4</sub> over ceria-supported metal catalysts." *Catalysis Today* **84**: 27-31.
- Cui, Y., H. Zhang, H. Xu and W. Li (2007). "Kinetic study of the catalytic reforming of CH<sub>4</sub> with CO<sub>2</sub> to syngas over Ni/[alpha]-Al<sub>2</sub>O<sub>3</sub> catalyst: The effect of temperature on the reforming mechanism." *Applied Catalysis A: General* **318**: 79-88.
- Dias, J. A. C. and J. M. Assaf (2008). "Autothermal reforming of methane over Ni/[gamma]-Al<sub>2</sub>O<sub>3</sub> promoted with Pd: The effect of the Pd source in activity, temperature profile of reactor and in ignition." *Applied Catalysis A: General* **334**(1-2): 243-250.
- Fogler, H. (1999). *Element of Chemical Reaction Engineering*, Prentice Hall PTR.
- Hardiman, K. M., F. J. Trujillo and A. A. Adesina (2005). "Deactivation-influenced propane steam reforming: reactor analysis and parameter estimation." *Chemical Engineering and Processing* **44**(9): 987-992.
- Kugai, J., V. Subramani, C. Song, M. H. Engelhard and Y.-H. Chin (2006). "Effects of nanocrystalline CeO<sub>2</sub> supports on the properties and performance of Ni-Rh bimetallic catalyst for oxidative steam reforming of ethanol." *Journal of Catalysis* **238**(2): 430-440.
- Levenspiel, O. (1999). "Chemical Reaction Engineering." *Ind. Eng. Chem. Res.* **38**(11): 4140-4143.
- Ma, L., A. A. Adesina and D. Trimm (1996). *Coking Resilience of Ceria-promoted Ni-based Steam Reforming Catalysts*. June 26-28, Beijing, P. R. China, Asian-Pacific Chemical Reaction Engineering Forum.

- Olafsen, A., A. Slagtern, I. M. Dahl, U. Olsbye, Y. Schuurman and C. Mirodatos (2005). "Mechanistic features for propane reforming by carbon dioxide over a Ni/Mg(Al)O hydrotalcite-derived catalyst." Journal of Catalysis **229**(1): 163-175.
- Solymosi, F., P. Tolmascov and T. S. Zakar (2005). "Dry reforming of propane over supported Re catalyst." Journal of Catalysis **233**(1): 51-59.
- Trovarelli, A., M. Boaro, E. Rocchini, C. de Leitenburg and G. Dolcetti (2001). "Some recent developments in the characterization of ceria-based catalysts." Journal of Alloys and Compounds **323-324**: 584-591.
- Wang, L., K. Murata and M. Inaba (2005). "Steam reforming of gasoline promoted by partial oxidation reaction on novel bimetallic Ni-based catalysts to generate hydrogen for fuel cell-powered automobile applications." Journal of Power Sources **145**(2): 707-711.
- Yaluris, G., R. B. Larson, J. M. Kobe, M. R. Gonzalez, K. B. Fogash and J. A. Dumesic (1996). "Selective Poisoning and Deactivation of Acid Sites on Sulfated Zirconia Catalysts for n-Butane Isomerization." Journal of Catalysis **158**(1): 336-342.
- Zhang, Z. L. and X. E. Verykios (1994). "Carbon dioxide reforming of methane to synthesis gas over supported Ni catalysts." Catalysis Today **21**: 589-595.